

ATOMIC PHYSICS WITH THE GODDARD HIGH RESOLUTION SPECTROGRAPH ON THE *HUBBLE SPACE TELESCOPE*. IV. RELATIVE OSCILLATOR STRENGTHS FOR SINGLY IONIZED NICKEL¹

J. ZSARGÓ² AND S. R. FEDERMAN³

Department of Physics and Astronomy, University of Toledo, Toledo, OH 43606

Received 1997 August 11; accepted 1997 December 4

ABSTRACT

Absorption lines of trace metals like nickel are often used to measure the metallicity and depletion in H I regions within our Galaxy and others. Ultraviolet absorption lines from the dominant ion, Ni II, are generally weak, making them a convenient tool to study metallicity and depletion in these environments. As an aid for studies of dust evolution in galaxies, we obtained an adjusted set of precise relative oscillator strengths for Ni II lines occurring at ultraviolet wavelengths. This set of f -values was derived from curves of growth for interstellar absorption toward ρ Oph A, χ Oph, and ζ Oph. In all, absorption from 12 lines was analyzed. Comparison with the compilation of Morton reveals good agreement for the stronger lines but significant differences for the weakest ones.

Subject heading: atomic data — ISM: abundances — ultraviolet: ISM

1. INTRODUCTION

Observations of trace metals like nickel or zinc provide an opportunity to study the chemical and dust evolution of galaxies. With ionization potentials of 18.17, 16.5, and 17.96 eV, Ni II, Cr II, and Zn II are the dominant ions of Ni, Cr, and Zn in H I regions. Although the former two are known to be heavily depleted onto dust grains, at least in the Galactic interstellar medium (Cowie & Songaila 1986), observations of interstellar Zn II have revealed little, if any, depletion. Numerous investigators have attempted to quantify the reliability of Zn II as a metallicity indicator through observations using the *International Ultraviolet Explorer* (York & Jura 1982; Harris, Bromage, & Blades 1983; Harris & Mas Hesse 1986; Van Steenberg & Shull 1988), *Copernicus* (Morton 1975, 1978), the Balloon-borne Ultraviolet Stellar Spectrometer (de Boer et al. 1986), and the *Hubble Space Telescope* (*HST*; Roth & Blades 1995; Sembach et al. 1995). These studies conclude that zinc may be depleted out of the gas phase by 30%–50% with respect to the solar abundance in Galactic interstellar material, with a potential increase noted for sight lines with larger $E(B - V)$, average particle density $n(\text{H})$, or molecular hydrogen fraction $f(\text{H}_2) = N(\text{H}_2)/[2N(\text{H}_2) + N(\text{H I})]$, where the last quantity provides a measure of gas/dust interaction (Cardelli 1994). However, the logarithmic gas-phase abundance of zinc, $(\text{Zn}/\text{H}) = \log [N(\text{Zn})/N_{\text{total}}(\text{H})] - \log (\text{Zn}/\text{H})_{\odot}$, is relatively constant with an average value of -0.19 ± 0.04 for sight lines where the fraction of molecular hydrogen is low [$f(\text{H}_2) \leq 10^{-3}$]. Consequently, zinc is a good measure of metallicity for galaxian gas with low molecular abundances. Studies of other species, like Si, Mg, Cr, Fe, and Ni, reveal considerable depletion onto dust grains even for gas in the Galactic halo (Sembach & Savage 1996). Of these elements, nickel shows the largest range in depletion from low-density to molecular-rich gas and therefore may be the best probe for grain evolution in galaxies.

Assuming the physical circumstances and chemistry of our Galaxy are uniform and representative, the $N(\text{Zn II})/N(\text{H I})$ ratio should be an effective measure of the metallicity in a distant galaxy as long as its molecular abundance is low. Attempts to detect H_2 in damped Ly α systems in QSO absorption spectra—which are believed to be caused by distant galaxies at high redshift—yield negligible amounts of molecules. The molecular fraction of hydrogen is found to be less than 10^{-3} (Levshakov et al. 1992). Thus the ratio $N(\text{Ni II})/N(\text{Zn II})$ or $N(\text{Cr II})/N(\text{Zn II})$ provides information on the dust content of such galaxies. Furthermore, the Ni II, Cr II, and Zn II absorption lines are expected to be weak, and therefore corrections for optically thick lines are a minor concern for these investigations.

The abundance ratios of Ni II, Cr II, and Zn II have been used in the study of damped Ly α systems observed in QSO absorption spectra (Meyer & York 1987; Meyer, Welty, & York 1989; Meyer & Roth 1990; Wolfe et al. 1994). The damped Ly α systems are most likely caused by intervening galaxies, since their H I column densities are comparable to interstellar sight lines through the disk of our Galaxy. Although the morphological interpretation of these intervening systems as galactic disks, their progenitors (Wolfe 1988), or gas-rich dwarf galaxies (York et al. 1986; Tyson 1988) is somewhat uncertain, they provide a unique opportunity to establish a chemical and dust evolutionary sequence for galaxies at large redshift. Such analyses, relying on Ni II, Cr II, and Zn II abundances, can have a subtle source of uncertainties beyond the obvious measurement errors. Most of the weak Ni II lines, for example, have no well-defined or measured oscillator strength (see Morton 1991). As long as the signal-to-noise ratio of the observations is low, the uncertainties are dominated by the measurement errors, but for observations with high signal-to-noise ratios, the precision in oscillator strengths is the controlling factor.

Here we improve the situation by providing a self-consistent set of relative oscillator strengths for Ni II lines in the range of 1300–1750 Å from measurements taken with the Goddard High Resolution Spectrograph (GHRS) on the *HST*. A combined curve-of-growth analysis of several lines of sight yields adjusted sets of oscillator strengths (Federman & Cardelli 1995; Zsargó, Federman, & Cardelli

¹ Based on observations obtained with the NASA/ESA *Hubble Space Telescope* through the Space Telescope Science Institute, which is operated by the Association of Universities for Research in Astronomy, Inc., under NASA contract NAS5-26555.

² jzsargo@utphys.phya.utoledo.edu

³ sfederm@uoft02.utoledo.edu

TABLE 1
 Ni II DATA

WAVELENGTH (Å)	W_λ (mÅ)				
	ρ Oph A ^a	χ Oph		ζ Oph	
		Component A ^b	Component B ^c	Component A ^b	Component B ^c
1345.878.....	0.69 ± 0.14^d	1.03 ± 0.27^d
1370.132.....	6.16 ± 0.38^e	8.92 ± 0.54^e
1393.324.....	7.31 ± 0.60	1.24 ± 0.30	2.57 ± 0.30
1412.866.....	2.84 ± 0.37
1415.720.....	2.68 ± 0.41
1449.997.....	1.32 ± 0.33	0.20 ± 0.08^d	0.34 ± 0.16^d
1454.842.....	17.85 ± 0.28	3.51 ± 0.21	6.22 ± 0.21	3.28 ± 0.21^d	4.19 ± 0.13^d
1467.259.....	5.48 ± 0.22	0.70 ± 0.16	1.58 ± 0.16	0.51 ± 0.12^d	0.68 ± 0.15^d
1467.756.....	8.36 ± 0.29	1.16 ± 0.19	2.37 ± 0.19	0.90 ± 0.15^d	1.45 ± 0.15^d
1477.222.....	0.91 ± 0.21
1709.600.....	4.97 ± 0.61^e	6.36 ± 0.67^e
1741.549.....	6.18 ± 0.78^e	7.17 ± 0.95^e

^a The measured total equivalent width.

^b Bluer component.

^c Redder component.

^d From Federman et al. 1993.

^e From Savage et al. 1992.

1997) if the uncertainties are dominated by the errors in the atomic properties. We used GHRS spectra of high quality with signal-to-noise ratios greater than 100–200 (Cardelli & Ebbets 1994; Fitzpatrick & Spitzer 1994; Lambert et al. 1994) to perform such an analysis. In § 2 we describe the measurements used in our analysis and outline the procedure used to obtain the new set of relative oscillator strengths in § 3. We describe the results in § 4 and make suggestions for further studies.

2. MEASUREMENTS

Our GHRS observations of ρ Oph A and χ Oph with grating G160M covered the range 1385–1488 Å. In all, eight Ni II lines toward ρ Oph A and four toward χ Oph could be identified (see Table 1). Two main interstellar absorption components with a separation of about 5 km s^{-1} are seen in Ca II K, Na D₁, and K I $\lambda 7699$ toward ρ Oph A (Hobbs 1975). The two components are not discerned in our *HST* spectra with a resolution of 15 km s^{-1} . As the determination of equivalent width (W_λ) for each component was impossible, we had to follow an iterative procedure to separate their contributions (see § 3). For χ Oph, the two main components with a separation of about 10 km s^{-1} were partially resolved, and individual values of W_λ could be determined with procedures available in NOAO's IRAF package. These data for the gas toward ρ Oph A and χ Oph were supplemented by measurements of eight Ni II absorption lines toward ζ Oph (see Table 1) taken from the literature (Savage, Cardelli, & Sofia 1992; Federman et al. 1993).

3. ANALYSIS

In order to obtain column densities [$N(X)$] and Doppler parameters (b -values), we performed curve-of-growth (COG) analyses (see Zsargó et al. 1997). In brief, we assumed simple Maxwellian line profiles to find the theoretical curve of growth because most lines had modest or negligible optical depths at line center. Values for N and b were obtained by least-squares fit, where the data for each line were weighted by the relative uncertainty in

$W_\lambda[\sigma(W_\lambda)/W_\lambda]$ and in the f -value.⁴ We divided our procedure into two parts. First, a complete analysis for the Ni II lines toward χ Oph and ζ Oph (including the determination of N and b , and the adjustment of f -values from the values given by Morton 1991) was performed. Then we incorporated the data for ρ Oph A into the procedure using the adjusted set of oscillator strengths. The adjusted f -values were used to produce synthetic profiles of the Ni II lines seen toward ρ Oph A in order to extract information about the two unresolved components. The last step involved a final adjustment to the set of f -values for the complete set of data.

The first analysis was straightforward. With the measured values of W_λ for each component toward χ Oph and ζ Oph, we obtained column densities and Doppler parameters. Since most of our measurements lie on the linear part of the curve of growth, the b -values are ill defined (see Figs. 1a and 1b). Instead, the least-squares fit was performed with one free parameter, the column density; the Doppler parameter was held constant. This restriction did not affect the reliability of our new set of oscillator strengths seriously ($\leq 10\%$ error in the case of the strongest lines). For the blue component associated with warm atomic gas (Savage et al. 1992), we chose a b -value of 3 km s^{-1} . The b -value for the redder component, which contains most of the material along the line of sight, was set at 1.5 km s^{-1} , a value consistent with results for other dominant ions (see Savage et al. 1992). Our column densities for the blue and red components toward χ Oph are $N(\text{blue}) = 3.76 \times 10^{12} \text{ cm}^{-2}$ and $N(\text{red}) = 8.58 \times 10^{12} \text{ cm}^{-2}$; those toward ζ Oph are $N(\text{blue}) = 3.13 \times 10^{12} \text{ cm}^{-2}$ and $N(\text{red}) = 4.28 \times 10^{12} \text{ cm}^{-2}$. The uncertainties in column densities are approximately 30% (3σ errors). These values are only meaningful for assessing the goodness of the fit and cannot represent actual column densities until the f -values are placed on an absolute scale with precise laboratory measurements. The

⁴ No quantified uncertainties in the oscillator strengths were given for most of the Ni II lines in Morton's (1991) compilation. We set the uncertainties to 30% in such cases, which proved to be reasonable in light of the correspondence between our results and the f -values in Morton (1991); see Table 2.

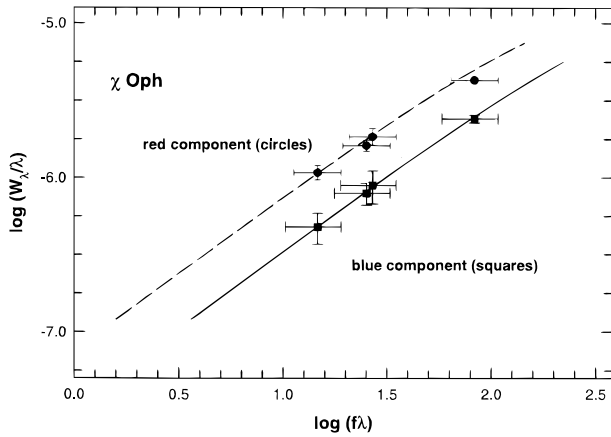


FIG. 1a

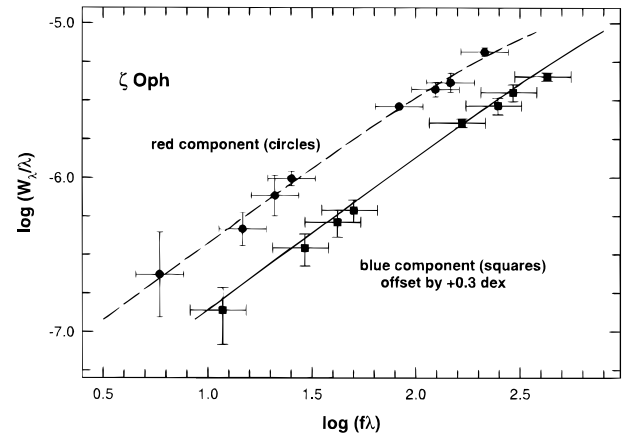


FIG. 1b

FIG. 1.—(a) Shows the curves of growth for the bluer (*filled squares*) and redder (*filled circles*) component toward χ Oph, utilizing the final set of adjusted oscillator strengths. The solid and dashed lines represent the corresponding theoretical curves of growth. It is clear that our measurements covered only the linear part of the curves of growth. (b) Same as (a) for the line of sight toward ζ Oph. For easier viewing, the blue component results were shifted by +0.3 dex in (b).

shape of the curves of growth, however, is not affected by the lack of an absolute scale in f -values, and therefore our analyses provide an accurate set of relative oscillator strengths.

Once we have COGs for all components toward χ Oph and ζ Oph, we can follow a procedure described by Zsargó et al. (1997) to adjust the f -values. Since our measurements are of very good quality, we assume that the deviations from the theoretical curve are due to inaccuracies in atomic properties. With several theoretical curves available (for separate components along different lines of sight) we can find adjusted, self-consistent oscillator strengths by minimizing the total deviation. A simple interactive data language routine was developed to carry out this procedure and was used previously to adjust C I oscillator strengths (see Zsargó et al. 1997). Here it is applied to the data on Ni II lines, where each line is treated separately. Figures 1a and 1b show the resultant curves of growth for the gas toward χ Oph and ζ Oph, respectively.

This initial set of adjusted oscillator strengths was used to synthesize the two unresolved components toward ρ Oph A. Two computer-generated components, each with an assumed Voigt profile convolved with the appropriate instrumental function, were fitted to each measured Ni II absorption line. Out of five unknown parameters (two column densities, two Doppler parameters, and the separation of components), only the two column densities were allowed to vary freely. The 5 km s^{-1} separation between components followed from the higher resolution results for Ca II K, Na D₁, and K I $\lambda 7699$ (Hobbs 1975). The b -value of the bluer component—like those for the other stars—was set to 3 km s^{-1} , while the redder one had $b = 2 \text{ km s}^{-1}$, based on results for C I (see Zsargó et al. 1997). The column densities were found by the best simultaneous fit to all available Ni II lines toward ρ Oph A. Figures 2a and 2b illustrate the respective results of the profile synthesis for a weak and a strong line.

The column density of the bluer component was found to be 20%–30% of the redder component, consistent with the observations of Ca II K, Na D₁, and K I $\lambda 7699$ (Hobbs 1975). The 15 km s^{-1} resolution of our spectra is coarse enough to question the reliability of these results, and thus we tested the effects of slightly different Doppler parameters

and separation. All of the trial runs showed that the bluer component is significantly smaller than the redder one.

Since the uncertainties in the resulting column densities were also approximately 30% for the stronger component,

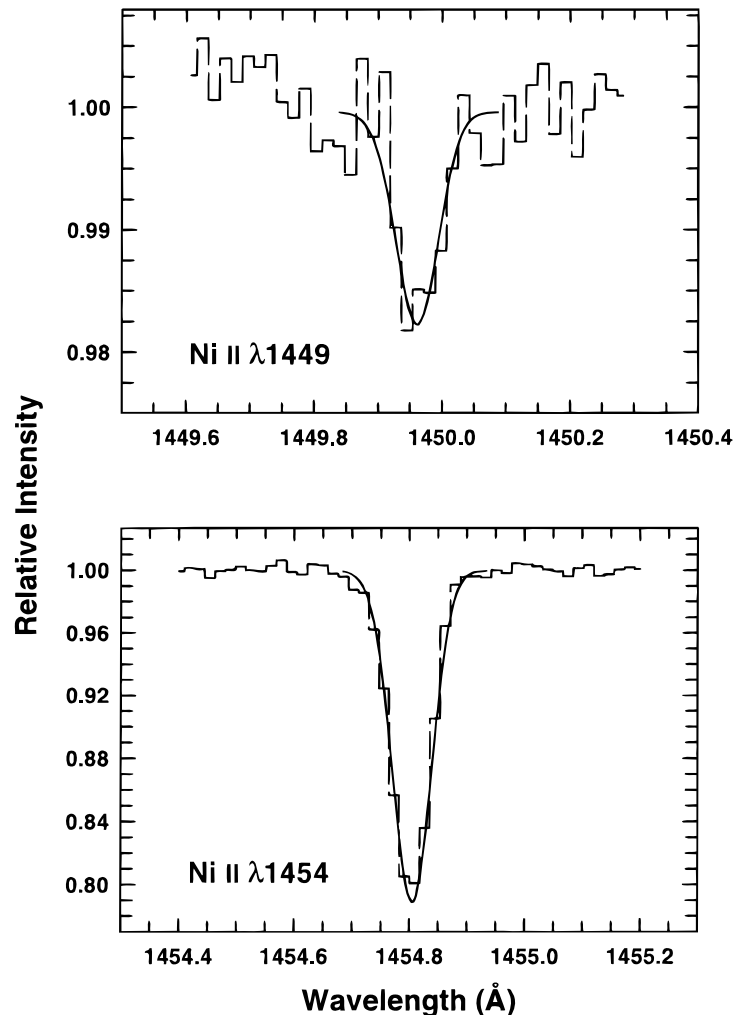


FIG. 2.—(a) Shows the synthesized (*smooth curve*) and observed profile for $\lambda 1450$. The synthesized profile is a superposition of two components. (b) Same as (a) for the stronger line at 1454 \AA .

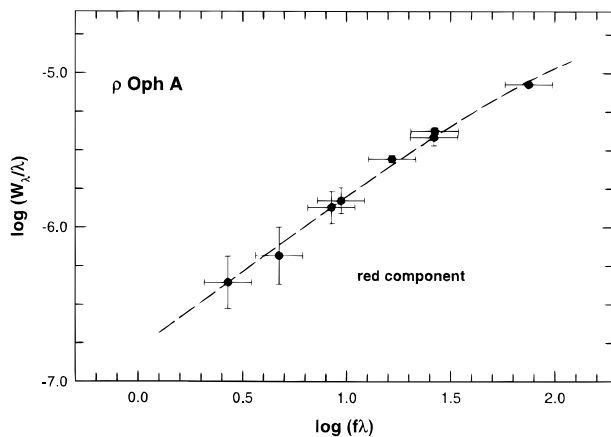


FIG. 3.—Same as Fig. 1a, but only the stronger (redder) component toward ρ Oph A is shown.

we decided not to involve the bluer component toward ρ Oph A in the final combined curve-of-growth analysis. As the optical depth at line center was small for both components and for most of our lines ($\tau_0 \leq 1.11$), the total equivalent width was approximated by the sum of the contributions from the two components. The total W_λ was measured with the IRAF package, and the W_λ for the stronger component (redder one) was obtained by subtracting the W_λ for the bluer component derived from its synthesized column density. The stronger component toward ρ Oph A, together with the components toward χ Oph and ζ Oph, was then incorporated into a combined COG analysis that yielded a new set of relative oscillator strengths. With this new set we could refine the W_λ of the stronger component toward ρ Oph A by repeating the outlined procedure. After two iterations the changes in f -value and W_λ were much less

TABLE 2
Ni II OSCILLATOR STRENGTHS

WAVELENGTH (Å)	$f(M)^a$	$f(ZsF)^b$	$f(M)/f(ZsF)$
1345.878.....	6.43(-3) ^c	1.44(-2)	0.447
1370.132.....	1.31(-1)	1.44(-1)	0.910
1393.324.....	2.22(-2)	1.89(-2)	1.175
1412.866.....	6.65(-3)	6.65(-3)	1.000
1415.720.....	4.13(-3)	5.97(-3)	0.692
1449.997.....	3.53(-3)	3.27(-3)	1.080
1454.842.....	5.95(-2)	5.16(-2)	1.153
1467.259.....	1.11(-2)	1.13(-2)	0.982
1467.756.....	2.27(-2)	1.81(-2)	1.254
1477.222.....	1.06(-3)	1.82(-3)	0.582
1709.600.....	6.88(-2)	6.66(-2)	1.033
1741.549.....	1.04(-1)	7.76(-2)	1.340

^a Morton 1991.

^b Present compilation.

^c $6.43(-3) = 6.43 \times 10^{-3}$.

than the uncertainties. The Doppler parameter of the COG for ρ Oph A was set at 2 km s^{-1} throughout the iterative analysis. The final column density for ρ Oph A was $N(\text{red}) = 1.87 \times 10^{13} \text{ cm}^{-2}$ (see Fig. 3 for the curve of growth for this component toward ρ Oph A). We note that the results for the stronger component toward ρ Oph A were weighted somewhat more heavily than the results for the four other components in the final step because its values for W_λ were larger, while the uncertainties were comparable. For the five lines in common, the f -values changed by less than 17% between this last step and the previous one without the data for ρ Oph A. The uncertainties in the derived f -values are somewhat high ($\approx 30\%$), but they have been quantified for the first time (see Table 2).

4. DISCUSSION

Table 2 shows the adjusted oscillator strengths together with their previous values (Morton 1991). The adjusted and the original f -values differ by less than 30% in most cases, implying that the theoretical calculations of Kurucz (1989) are reliable (in a relative sense). There are several lines with considerable differences: the oscillator strength of $\lambda 1345$ has changed by more than 100% and those of $\lambda\lambda 1477$, 1415 by more than 70% and by about 40%, respectively. Unfortunately we measured these lines in only one direction, which could result in higher than average uncertainties. These three lines are among the weakest observed by us, and it is not unreasonable to find the largest discrepancies here between our results and the predictions of Kurucz (1989, private communication) from intermediate coupling calculations. We also note that our f -value for $\lambda 1345$ agrees with the one deduced by Federman et al. (1993)—0.0140—from a less sophisticated analysis.

In conclusion, precise relative f -values for 12 ultraviolet lines in the spectrum of Ni II were derived from interstellar observations. Ours is the first empirical measure for this set of lines. The relative strengths for the stronger lines are consistent with the results listed in Morton's (1991) compilation, but revisions are suggested for several weak transitions. In order to place our results on an absolute scale, accurate laboratory results are needed; we are now preparing to carry out such an experiment. In the meantime, the set of relative f -values presented here allows analyses of nickel depletion in interstellar environments to have a common basis, even when different lines are observed.

This research was supported by NASA grant NAGW-3840 and STScI grant GO-05389.02-93A. We are grateful to Yaron Sheffer, who provided the profile-fitting code for our analysis, and to Lew Hobbs for copies of his data files. We thank Dave Ellis and Dick Schectman for their comments on an earlier draft.

REFERENCES

- Cardelli, J. A. 1994, *Science*, 265, 209
 Cardelli, J. A., & Ebbets, D. C. 1994, in *HST Calibration Workshop, Calibrating Hubble Space Telescope*, ed. J. C. Blades & A. J. Osmer (Baltimore: STScI), 322
 Cowie, L. L., & Songaila, A. 1986, *ARA&A*, 24, 499
 de Boer, K. S., Lenhart, H., van der Hucht, K. A., Kamperman, T. M., Kondo, Y., & Bruhweiler, F. C. 1986, *A&A*, 157, 119
 Federman, S. R., & Cardelli, J. A., 1995, *ApJ*, 452, 269
 Federman, S. R., Sheffer, Y., Lambert, D. L., & Gilliland, R. L. 1993, *ApJ*, 413, 51
 Fitzpatrick, E. L., & Spitzer, L. 1994, *ApJ*, 427, 232
 Harris, A. W., Bromage, G. E., & Blades, J. C. 1983, *MNRAS*, 203, 1225
 Harris, A. W., & Mas Hesse, J. M. 1986, *MNRAS*, 220, 271
 Hobbs, L. M. 1975, *ApJ*, 200, 621
 Lambert, D. L., Sheffer, Y., Gilliland, R. L., & Federman, S. R. 1994, *ApJ*, 420, 756
 Levshakov, S. A., Chaffee, F. H., Foltz, C. B., & Black, J. H. 1992, *A&A*, 262, 385
 Meyer, D. M., & Roth, K. C. 1990, *ApJ*, 268, 76
 Meyer, D. M., Welty, D. E., & York, D. G. 1989, *ApJ*, 343, L37
 Meyer, D. M., & York, D. G. 1987, *ApJ*, 319, L45
 Morton, D. C. 1975, *ApJ*, 197, 85

- Morton, D. C. 1978, *ApJ*, 222, 863
———, 1991, *ApJS*, 77, 119
- Roth, K. C., & Blades, J. C. 1995, *ApJ*, 445, L95
- Savage, B. D., Cardelli, J. A., & Sofia, U. J. 1992, *ApJ*, 401, 706
- Sembach, K. R., & Savage, B. D. 1996, *ApJ*, 457, 211
- Sembach, K. R., Steidel, C. C., Macke, R. J., & Meyer, D. M. 1995, *ApJ*, 445, L27
- Tyson, N. D. 1988, *ApJ*, 329, L57
- Van Steenberg, M. E., & Shull, J. M. 1988, *ApJ*, 330, 942
- Wolfe, A. M. 1988, in *QSO Absorption Lines: Probing the Universe*, ed. J. C. Blades, D. A. Turnshek, & C. A. Norman (Cambridge: Cambridge Univ. Press), 297
- Wolfe, A. M., Fan, X.-M., Tytler, D., Vogt, S. S., Keane, M. J., & Lanzetta, K. M. 1994, *ApJ*, 435, L101
- York, D. G., Dopita, M., Green, R. F., & Bechtold, J. 1986, *ApJ*, 311, 610
- York, D. G., & Jura, M. 1982, *ApJ*, 254, 88
- Zsargó, J., Federman, S. R., & Cardelli, J. A. 1997, *ApJ*, 484, 820